Lateral Structure Interaction With Seismic Waves

R. J. SCAVUZZO
Associate Professor of Mechanical Engineering, Hartford Graduate Center, Rensselaer Polytechnic Institute, East Windsor Hill, Conn. Mem. ASME

J. L. BAILEY
Associate Professor, Department of Mathematics.

D. D. RAFTOPOULOS
Associate Professor, Department of Mechanical Engineering. Mem. ASME

The University of Toledo, Toledo, Ohio

The interaction of lateral structural inertia forces with horizontal seismic motion is formulated in terms of an integral equation of the Volterra type. By means of normal mode theory the inertia force at the base of the structure is expressed as a function of the foundation motion. After the motion of the two-dimensional elastic half space resulting from a uniform horizontal foundation force varying arbitrarily with time over a specified interval on the boundary of the half space has been determined, the interaction equation is derived. Numerical studies for two free-field acceleration inputs are made for different ground stiffnesses and structural characteristics. The first of these free-field inputs is a ramp sine function and the second is the east-west ground acceleration recorded at Golden Gate Park during the 1957 San Francisco earthquake. The interaction effects for structures similar to nuclear power plants prove to be significant.

Introduction

During seismic motions caused by earthquake or explosive forces, inertia loads of large building structures tend to resist the foundation movement. Since the earth is flexible, these inertia forces will change the seismic motions locally from free-wave values. Lateral and vertical free-field motions will be altered and structure rocking will be initiated.

One of the first attempts to analyze this interaction problem was made by Jacobsen [1][1] in 1938. However, in this study, the dynamic characteristics of the half space were approximated. Biot [2] published one of the first papers in which a spectrum approach was proposed for engineering seismic analysis. In this paper, Biot discussed the interaction problem and stated that in certain cases this "stress-reducing factor" may become very large. Since that time many researchers have contributed toward the solution of this problem [3]. The significance of interaction effects in an engineering problem was first evaluated on underwater shocks by Belsheim, Blake, and O'Hara and others at the Naval Research Laboratory [4–15]. In the field of earthquake engineering recent contributions have been made by Parmalee [16], Luco [17] and Agabein, et al. [18]. Parmalee coupled an N-mass structure to a half space. The half-space analysis was based on Bycroft's steady-state solution [19, 20]. Interaction effects of a number of conventional multistory building structures were studied. Luco investigated the interaction of a shear wall with the soil using a harmonic incident wave. The magnitude of the base shear force was shown to be dependent on the input wave frequency. At resonance, interaction effects greatly limited the magnitude of the base shear force. Agabein, Parmalee, and Lee developed a lumped parameter mathematical model for a study on soil-structure interaction. It was concluded by the authors that ". . . the influence of flexibility of the foundation on the seismic response of the multistory building is significant. . . ." Effects on the base spectrum response caused by interaction were not thoroughly investigated in these studies. In 1967 Scavuzzo [21] analyzed the interaction between the lateral foundation motion of large structures and lateral seismic motion at the base by means of a one-dimensional modeling of the earth. Although the oversimplification of the earth model precluded the possibility of analyzing the effects of the shear and Rayleigh waves, this paper provided a basis for predicting the interaction effects to be significant. Similar techniques have also been applied to the underwater shock problem [22].

In this investigation, the effects of interaction between lateral inertia forces and lateral foundation motions are considered for a two-dimensional model of the earth. The two-dimensional model permits inclusion of the shear and Rayleigh wave effects. The significance of this interaction effect is evaluated by noting changes in spectrum responses from values obtained without any structure present. Changes in lateral acceleration at the foundation of a structure from free-field accelerations are also presented. Interaction effects caused by vertical motion, torsion, rocking, and large base masses have been deferred.

[1] Numbers in brackets designate References at end of paper.

Presented at the Sixth U. S. National Congress of Applied Mechanics, Harvard University, Cambridge, Mass., June 15–19, 1970.

Discussion of this paper should be addressed to the Editorial Department, ASME, United Engineering Center, 345 East 47th Street, New York, N. Y. 10017, and will be accepted until April 20, 1971. Discussion received after the closing date will be returned. Manuscript received by ASME Applied Mechanics Division, November 26, 1969; final revision, April 24, 1970.

Theory[2]

Foundation Inertial Force. Inertia forces at the base of a structure that can be idealized as an N-mass system can be expressed as a function of the lateral base acceleration $\ddot{u}(0, 0, t)$, the natural frequencies of vibration ω_j, and the effective model mass M_j [4, 5].

$$F(t) = -\sum_j M_j\omega_j \int_0^t \ddot{u}(0, 0,\tau) \sin \omega_j(t - \tau)d\tau \tag{1}$$

The effective mass is defined by

$$M_j = \frac{\left(\sum_i \bar{X}_{ij}m_i\right)^2}{\sum_i \bar{X}_{ij}^2 m_i} \tag{2}$$

where $\bar{X}_{ij}$ are the mode shapes (eigenvectors) of the linear elastic N-mass structure fixed at the base and m_i are the concentrated masses.

Solution to Lamb's Problem. The solution is derived for the lateral displacements at the origin for a two-dimensional homogeneous elastic half space where the stress distribution on the surface is prescribed by a zero normal stress and a shear stress that varies arbitrarily with time in the interval $-c < x < c$ and is zero outside of this interval, Fig. 1. Transform techniques are used to obtain the solution. The infinite Fourier transform with respect to x and the Laplace transform with respect to t are applied. This procedure follows the method described by Flitman [23].

For dynamic elasticity problems in two dimensions, the equations of motion can be expressed as

$$\rho\frac{\partial^2 u}{\partial t^2} = (\lambda + \mu)\left(\frac{\partial^2 u}{\partial x^2} + \frac{\partial^2 v}{\partial x\partial y}\right) + \mu\nabla^2 u$$
$$\rho\frac{\partial^2 v}{\partial t^2} = (\lambda + \mu)\left(\frac{\partial^2 u}{\partial x\partial y} + \frac{\partial^2 v}{\partial y^2}\right) + \mu\nabla^2 v \tag{3}$$

By introducing the two scalar functions ϕ and ψ such that $u = \frac{\partial\phi}{\partial x} + \frac{\partial\psi}{\partial y}$ and $v = \frac{\partial\phi}{\partial y} - \frac{\partial\psi}{\partial x}$ equations (3) can be written as

$$\frac{1}{a^2}\frac{\partial^2\phi}{\partial t^2} = \nabla^2\phi$$
$$\frac{1}{b^2}\frac{\partial^2\psi}{\partial t^2} = \nabla^2\psi \tag{4}$$

[2] See the Nomenclature for definitions of the symbols.

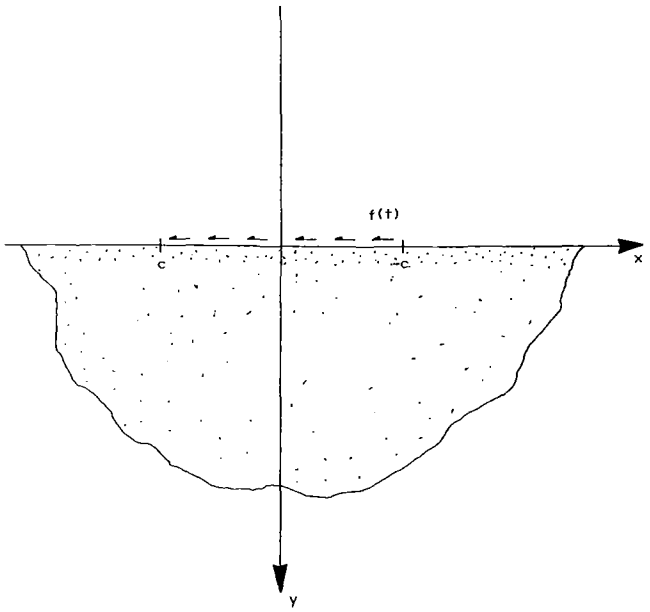

Fig. 1 Coordinate system used in solution to the Lamb problem. A shear stress, $f(t)$, which acts between $\pm c$ varies arbitrarily with time. The remaining portion of the surface is stress free. Normal stresses over the entire surface are zero.

By making use of Hooke's law, the stresses can be written as [24]

$$\sigma_x = 2\mu\left(\frac{\partial^2\phi}{\partial x^2} + \frac{\partial^2\psi}{\partial x\partial y}\right) + \lambda\nabla^2\phi$$
$$\sigma_y = 2\mu\left(\frac{\partial^2\phi}{\partial y^2} - \frac{\partial^2\psi}{\partial x\partial y}\right) + \lambda\nabla^2\phi \tag{5}$$
$$\tau_{xy} = \mu\left(2\frac{\partial^2\phi}{\partial x\partial y} + \frac{\partial^2\psi}{\partial y^2} - \frac{\partial^2\psi}{\partial x^2}\right)$$

The boundary conditions used in the solution are

$$\sigma_y = 0 \qquad y = 0$$
$$\tau_{xy} = \begin{cases} f(t), & |x| < c, \quad y = 0 \\ 0, & |x| > c, \quad y = 0 \end{cases} \tag{6}$$
$$\sigma_x = \sigma_y = \tau_{xy} = 0, \qquad y = \infty$$

Taking the Laplace and Fourier transforms of the ϕ and ψ functions defined by

Nomenclature

a = dilatation (P) wave velocity $a = \sqrt{\frac{\lambda + 2\mu}{\rho}}$
A = area of structure base
b = shear (S) wave velocity $b = \sqrt{\frac{\mu}{\rho}}$
c = half the length dimension of area in plane of the half space
E = Young's modulus
$F(t)$ = lateral force at base of a structure
$f(t)$ = surface shear stress when $|x| < c$
M_j = effective mass of jth mode
m_j = jth structure mass
p = transformed time variable
$u(x, y, t)$ = lateral displacement (x-direction)
$u(t)$ = lateral displacement of center of base
$u_p(t)$ = free-field lateral displacement at center of base
$v(x, y, t)$ = vertical displacement (y-direction)
V = Rayleigh wave velocity
$\bar{X}_{ij}$ = eigenvector corresponding to ith mass in jth mode
ω_j = natural circular frequency of jth mode
λ = Lamé constant $\lambda = \frac{\nu E}{(1 + \nu)(1 - 2\nu)}$
μ = shear modulus $\mu = \frac{E}{2(1 + \nu)}$
ν = Poisson's ratio
ξ = transformed x-coordinate
ρ = ground density
σ_x = tensile stress in the x-direction
σ_y = tensile stress in the y-direction
τ_{xy} = shear stress
ϕ = dilatation scalar potential
ψ = equivoluminal (shear) wave function
∇^2 = Laplace operator $\nabla^2 = \frac{\partial^2}{\partial x^2} + \frac{\partial^2}{\partial y^2}$

$$\bar{\bar{\phi}}(\xi, y, p) = \int_{-\infty}^{+\infty} e^{i\xi x} \int_0^{\infty} e^{-pt}\phi(x, y, t)dtdx$$
$$\bar{\bar{\psi}}(\xi, y, p) = \int_{-\infty}^{+\infty} e^{i\xi x} \int_0^{\infty} e^{-pt}\psi(x, y, t)dtdx \tag{7}$$

yields

$$\frac{d^2\bar{\bar{\phi}}}{dy^2} - \left(\xi^2 + \frac{p^2}{a^2}\right)\bar{\bar{\phi}} = 0$$
$$\frac{d^2\bar{\bar{\psi}}}{dy^2} - \left(\xi^2 + \frac{p^2}{b^2}\right)\bar{\bar{\psi}} = 0 \tag{8}$$

The double transform of the boundary condition on τ_{xy} can be expressed as

$$\bar{\bar{\tau}}_{xy}(\xi, 0, p) = \frac{2\bar{f}(p) \sin c\xi}{\xi} \tag{9}$$

By determining $\bar{\bar{\phi}}$ and $\bar{\bar{\psi}}$ the solution for the transformed displacement at $y = 0$ can be found.

$$\bar{\bar{u}}(\xi, 0, p) = -\frac{p^2\bar{f}(p) \sin c\xi \sqrt{\xi^2 + \frac{p^2}{b^2}}}{2b^2\mu\xi D(\xi, p)} \tag{10}$$

where

$$D(\xi, p) = \left(\xi^2 + \frac{p^2}{2b^2}\right)^2 - \xi^2\sqrt{\xi^2 + \frac{p^2}{a^2}}\sqrt{\xi^2 + \frac{p^2}{b^2}} \tag{11}$$

The solution for the displacements is obtained by taking the inverse transforms of $\bar{\bar{u}}$. From the Fourier inversion integral

$$\bar{u}(x, 0, p) = -\frac{p^2\bar{f}(p)}{4\pi b^2\mu}\int_{-\infty}^{\infty} \frac{\sqrt{\xi^2 + \frac{p^2}{b^2}} \sin c\xi}{\xi D(\xi, p)} e^{-i\xi x}d\xi \tag{12}$$

By equating $\sin c\xi$ to $\text{Im } e^{ic\xi}$ and x to zero and by halving the interval of integration and doubling the even integrand, the integral in the last equation becomes

$$2\int_0^{\infty} \frac{\sqrt{\xi^2 + \frac{p^2}{b^2}} \text{ Im } e^{ic\xi}}{\xi D(\xi, p)} d\xi = \text{Im}\left\{2\int_0^{\infty} \frac{\sqrt{\xi^2 + \frac{p^2}{b^2}}}{\xi D(\xi, p)} e^{ic\xi}\, d\xi\right\} \tag{13}$$

Like $\dfrac{\sqrt{\xi^2 + \frac{p^2}{b^2}}}{\xi D(\xi, p)}$ in the preceding equation, $\dfrac{p^2\bar{f}(p)}{4\pi b^2\mu}$ is real-valued and

$$\bar{u}(0, 0, p) = \text{Im}\left\{-\frac{p^2\bar{f}(p)}{2\pi b^2\mu}\int_0^{\infty} \frac{\sqrt{\xi^2 + \frac{p^2}{b^2}}}{\xi D(\xi, p)} e^{ic\xi}d\xi\right\} \tag{14}$$

By putting $ic\xi = -p\tau$ the integral can be written in a convenient form. This procedure was used by Chao in his solution of a similar three-dimensional problem [25]. Thus $\bar{u}$ can be rewritten as

$$\bar{u}(0, 0, p) = \text{Im}\left\{-\frac{b^2}{2\pi\mu c}\frac{\bar{f}(p)}{p}\int_0^{-i\infty} g\left(\frac{b\tau}{c}\right)e^{-p\tau}d\tau\right\} \tag{15}$$

where the integration takes place down the imaginary axis of the complex τ-plane and

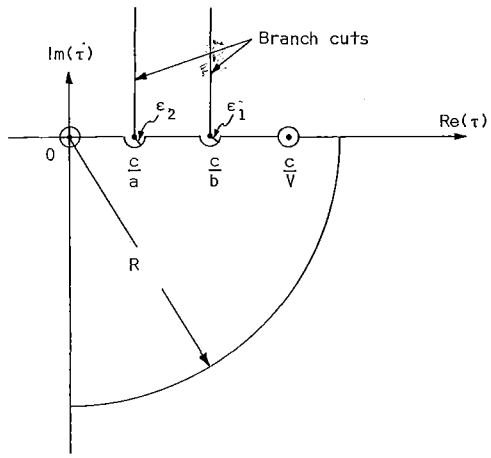

Fig. 2 Path of integration

$$g(T) = \frac{\sqrt{1 - T^2}}{T\left[\left(\frac{1}{2} - T^2\right)^2 + T^2\sqrt{\frac{b^2}{a^2} - T^2}\sqrt{1 - T^2}\right]} \tag{16}$$

It can be noted that $T^2 = \left(\dfrac{b\tau}{c}\right)^2$ is real-valued and nonpositive for τ on the imaginary axis and that all the square roots are real-valued nonnegative numbers. The integral appearing in equation (15) can be determined in terms of $L\left\{g\left(\dfrac{bt}{c}\right)\right\}$ from the evaluation of the Cauchy principal value of $\oint g\left(\dfrac{b\tau}{c}\right)e^{-p\tau}d\tau$ over the fourth-quadrant contour in Fig. 2 by means of the residue theorem modified to cover the case where simple poles lie on the countour.

The integrand of $\oint g\left(\dfrac{b\tau}{c}\right)e^{-p\tau}d\tau$ has branch points at $\tau = \pm\dfrac{c}{a}$ and $\tau = \pm\dfrac{c}{b}$, a simple pole at the origin, and, if Poisson's ratio is specialized to $1/4$, other simple poles at $\tau = \pm\dfrac{c}{V}$ where V, the speed of the Rayleigh wave, equals $\dfrac{2b}{\sqrt{3 + \sqrt{3}}}$ for a Poisson's ratio of $1/4$. From an elemental examination of g it is clear that $\pm(c/a)$ and $\pm(c/b)$ are branch points and that the origin is a simple pole. The other simple poles at $\pm(c/V)$ are determined as the zeros of the square-bracketed expression in the denominator of $g(T)$. In solving for these zeros by elementary algebra, it can be shown that for the zeros to be determined T^2 satisfies a cubic equation with roots $1/4$, $\dfrac{3 - \sqrt{3}}{4}$, and $\dfrac{3 + \sqrt{3}}{4}$ [26]. The first two of these roots are extraneous and the third corresponds to $\tau = \pm(c/V)$. The Cauchy principal value of the integral $\oint g\left(\dfrac{b\tau}{c}\right)e^{-p\tau}d\tau$ around the contour in Fig. 2 is written as the sum of integrals in the equation (17) and the modified residue theorem is used.

$$P\oint_C g\left(\frac{b\tau}{c}\right)e^{-p\tau}d\tau = \left(\frac{\pi}{2}\,i \underset{\tau=0}{\text{res}} + \pi i \underset{\tau=\frac{c}{V}}{\text{res}}\right)g\left(\frac{b\tau}{c}\right)e^{-p\tau} \tag{17}$$

where P denotes the Cauchy principal value of the integral and C is the contour in Fig. 2 traced in the counterclockwise direction. In the limit as $R \to \infty$, $\epsilon_1 \to 0$, and $\epsilon_2 \to 0$, all the integrals over the circular arcs in equation (17) vanish, three of the remaining integrals combine to give $-L\left\{g\left(\dfrac{bt}{c}\right)\right\}$, and equation (17) simplifies to

$$\int_0^{-i\infty} g\left(\frac{b\tau}{c}\right) e^{-p\tau} d\tau = L\left\{g\left(\frac{bt}{c}\right)\right\} + \left(\frac{\pi}{2} i \operatorname*{res}_{\tau=0} + \pi i \operatorname*{res}_{\tau=\frac{c}{V}}\right) g\left(\frac{b\tau}{c}\right) e^{-p\tau} \quad (18)$$

The residue at $t = 0$ is $(4c/b)$. The residue at $\tau = (c/V)$ is purely imaginary and therefore makes no contribution to the value of $\bar{u}(0, 0, p)$. Hence by use of equation (18), equation (15) can be rewritten as

$$\bar{u}(0, 0, p) = \operatorname{Im}\left\{-\frac{b^2}{2\pi\mu c}\frac{\bar{f}(p)}{p} L\left\{g\left(\frac{bt}{c}\right)\right\} - i\frac{b}{\mu}\frac{\bar{f}(p)}{p}\right\} \quad (19)$$

Application of the operational formula $L\left\{\int_0^t f(\eta)d\eta\right\} = \frac{\bar{f}(p)}{p}$ and the convolution theorem yields the final solution, $u(0, 0, t)$, of the original boundary-value problem.

$$u(0, 0, t) = -\frac{b}{\mu}\int_0^t f(\tau)d\tau - \frac{b^2}{2\pi c\mu} \times \int_0^t \int_0^{t-\tau} f(\xi) \operatorname{Im} g\left(\frac{b\tau}{c}\right) d\xi d\tau \quad (20)$$

where $\operatorname{Im} g\left(\frac{b\tau}{c}\right)$ is computed from equation (16) with $(a^2/b^2) = 3$ as is implied from assuming Poisson's ratio equal to $1/4$. The form of $\operatorname{Im} g(T)$ is given by equation (21).

$$\operatorname{Im} g(T) = \begin{cases} 0 & , 0 < T < \frac{1}{\sqrt{3}} \\ \dfrac{3T(1 - T^2)\sqrt{T^2 - \frac{1}{3}}}{2(T^2 - \frac{1}{4})\left(T^2 - \frac{3 - \sqrt{3}}{4}\right)\left(T^2 - \frac{3 + \sqrt{3}}{4}\right)} & , \frac{1}{\sqrt{3}} < T < 1 \\ -\dfrac{3\sqrt{T^2 - 1}\left\{(\frac{1}{2} - T^2)^2 + T^2\sqrt{T^2 - \frac{1}{3}}\sqrt{T^2 - 1}\right\}}{2T(T^2 - \frac{1}{4})\left(T^2 - \frac{3 - \sqrt{3}}{4}\right)\left(T^2 - \frac{3 + \sqrt{3}}{4}\right)} & , T > 1 \end{cases} \quad (21)$$

The integral in equation (20) is proper for $0 < t < \frac{c}{V}$. At $\tau = \frac{c}{V}$ $\operatorname{Im} g\left(\frac{b\tau}{c}\right)$ has a singular point of order $\left(\tau - \frac{c}{V}\right)^{-1}$. The displacement at $t = \frac{c}{V}$, however, is finite since the indeterminant form in the integrand, $\lim_{\tau \to \frac{c}{V}} \int_0^{\frac{c}{V} - \tau} \frac{f(\eta)d\eta}{\left(\tau - \frac{c}{V}\right)}$ exists. For $t > \frac{c}{V}$, because of the singular point at $\tau = \frac{c}{V}$, to be meaningful the integral in equation (20) must be considered as its Cauchy principal value. In which case $u(0, 0, t)$ is a well-defined finite value for all nonnegative t. The singularity at $\tau = \frac{c}{V}$ is expected in this kind of problem [25].

Interaction Equations. The total lateral displacement at the center of the base of the structure, $u(t)$, due to inertial shear stress of the structure and the free-field displacement, $u_p(t)$, is obtained by superposing on the solution of the half-space problem the free-field displacement, $u_p(t)$.

$$u(t) = -\frac{b}{\mu}\int_0^t f(\tau)d\tau - \frac{b^2}{2\pi c\mu} \times \int_0^t \int_0^{t-\tau} f(\xi) \operatorname{Im} g\left(\frac{b\tau}{c}\right) d\xi d\tau + u_p(t) \quad (22)$$

By taking the second time derivative in equation (22) and by substituting $f(t) = \frac{-F(t)}{A}$ with $F(t)$ written out as in equation (1), the following interaction equation can be obtained.

$$\ddot{u}(t) = -\frac{b}{\mu A}\sum_j M_j\omega_j^2 \int_0^t \ddot{u}(\xi) \cos\omega_j(t - \xi)d\xi - \frac{b^2}{2\pi\mu cA}\int_0^t \sum_j M_j\omega_j^2 \int_0^{t-\tau} [\ddot{u}(\xi) \cos\omega_j(t - \tau - \xi)d\xi] \times \operatorname{Im}\left(g\left(\frac{b\tau}{c}\right)\right) d\tau + \ddot{u}_p(t) \quad (23)$$

Equation (23) is an integral equation of the Volterra type in terms of the foundation acceleration $\ddot{u}(t)$ at the origin of the coordinate system. The prescribed function $\ddot{u}_p(t)$ is the lateral free-field acceleration at the origin without a structure present. In equation (23) the modal characteristics of the structure are described by the effective mass M_j and circular frequency ω_j for each (jth) mode of the system. Foundation geometry is defined by the base area A and the effective base half width c. The elastic properties of the ground are described by the shear velocity b and the shear modulus u.

Integral equation (23) is solved by classical iteration performed numerically at each time interval. A digital computer program listed in reference [27] can be used to input any digitized free-field value. Shock spectrum values are calculated for both free-field accelerations and foundation accelerations in a separate program. By comparing spectra at the mode frequencies the effects of lateral interaction on seismic loads can be evaluated for a given structure.

Discussion

Numerical studies are based on two different types of structures: a modern pressurized water nuclear power plant and a conventional 10-story building. A fixed-base fundamental frequency of 4.06 cps is calculated for the containment vessel of the plant under consideration. The fundamental frequency of the 10-story building is 0.8 cps. These two structures represent realistic extremes in dynamic response because the first structure is stiff and heavy and the second structure is relatively flexible.

The dynamic characteristics of the nuclear power plant are based upon a compact dynamic model which has been provided by the Stone and Webster Engineering Corporation of Boston, Mass., Fig. 3. It should be noted from Fig. 3 that the weight of the base mass is much greater than the dynamic masses. However, subsequent calculations show that spectrum values at the fixed-base frequencies are affected most significantly by the dynamic masses (28). Furthermore, in the numerical results presented herein, only the containment vessel dynamic mass is considered.

The Alexander building, a 10-story building located in San Francisco, Calif., which has been studied by seismic engineers for many years, is used as the second structure. Dynamic properties of this building have been determined by both test and analyses

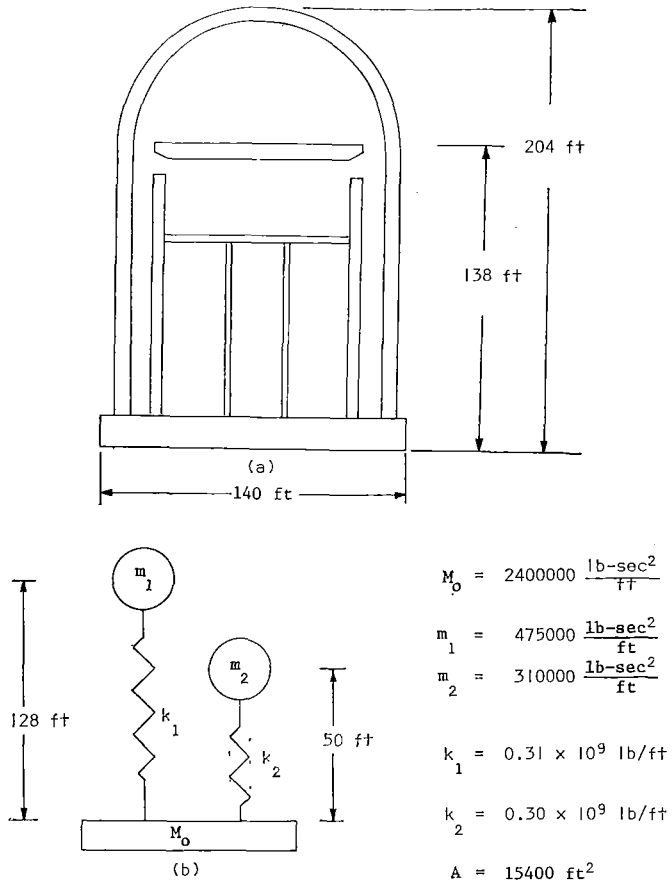

Fig. 3 Nuclear power plant shown in Fig. 2(*a*) has been idealized as indicated in Fig. 2(*b*). The masses M_0, m_1, and m_2 represent the base, containment vessel, and internal structure, respectively.

[29, 30]. Clough [30] reported the effective masses for the first three modes of vibration for a 10-mode dynamic model. In this paper, effective masses for the first three modes of a 10-mode dynamic model are reported. These effective masses (10,377,000 lb, 2,432,000 lb, and 595,000 lb, respectively) include 92 percent of the total weight (14,619,000 lb) and, therefore it should be a good dynamic model of the structure to study interaction effects. Natural frequencies of the first three modes are 0.8 cps, 2.8 cps and 5.0 cps, respectively. It should be noted that the fundamental frequency of this building is a factor of five lower than that of the nuclear containment structure.

Two free-field ground accelerations, $\ddot{u}_p(t)$ are used in these studies. In the first series a sinusoidal ramp function defined by equation (24) and plotted on Figs. 4 and 5 is prescribed.

$$u_p(t) = \begin{cases} \frac{5t}{8} \sin 10\pi t & 0 \le t \le 0.8 \\ 5\left(\frac{2-t}{14}\right) \sin 10\pi t & 0.8 < t \le 2.0 \\ 0 & t > 2.0 \end{cases} \tag{24}$$

Only the dynamic model based on the nuclear power plant is subjected to this input.

All mechanical properties of the half space can be defined by the shear wave velocity, the density, and Poisson's ratio. In all studies the ground density is taken to be 100 lb/ft³ and Poisson's ratio is made equal to 1/4. Thus the elastic ground properties are completely defined by the shear wave velocity. In all studies, shear wave velocities of 500 fps, 1000 fps, and 2000 fps are used as input. The lowest velocity is representative of soft soils; the highest velocity is representative of reasonably hard soils.

Initially, the single mass oscillation representing the containment vessel mass with a fixed base frequency of 4.06 cps was subjected to this ideal input. Calculated foundation accelerations for the case with a soil shear wave velocity of 2000 fps are shown in Fig. 4. In the next series of calculations, the frequency of the system is increased to 5 cps so that it is tuned to the frequency of the prescribed motion. Foundation accelerations for a soil shear wave velocity of 1000 fps are shown in Fig. 5. It should be noted that the foundation acceleration is initially in phase with the free-field acceleration and then becomes out-of-phase. This change in phase occurs with all three soil stiffnesses. Furthermore, resonance, as observed in forced mechanical vibrations, does not occur even though the structure has the same frequency as the input wave. This characteristic has been previously observed [21].

The engineering significance of these interaction effects is best evaluated by comparing the peak shock force felt by the structure when subjected to the free-field motion and calculated foundation motion. This peak force is proportional to the acceleration spectrum response evaluated at the natural frequency of the vibration mode under consideration [5, 12, 13]. Thus, by numerically performing the integration

$$s(\omega) = \frac{\omega}{g}\left(\int_0^t \ddot{u}(\tau) \sin \omega(t-\tau) d\tau\right)_{max} \tag{25}$$

the spectrum response in G's of acceleration can be calculated. In Fig. 6, the spectrum response of the free-field acceleration is shown as a solid line. In addition the spectrum values determined from the foundation accelerations calculated from equation (23) are plotted at frequencies of 4.06 cps and 5.0 cps for the three

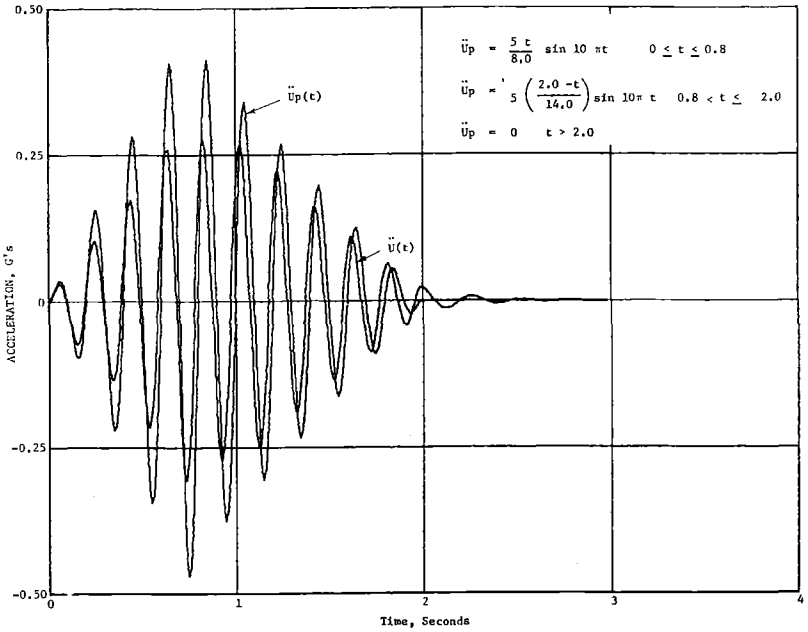

Fig. 4 The acceleration response of a single mass system weighing 475,000 slugs to a ramp sinusoidal function with a 5 cps is shown. The natural frequency of the system is 4.06 cps and the ground shear wave velocity was taken to be 1000 fps.

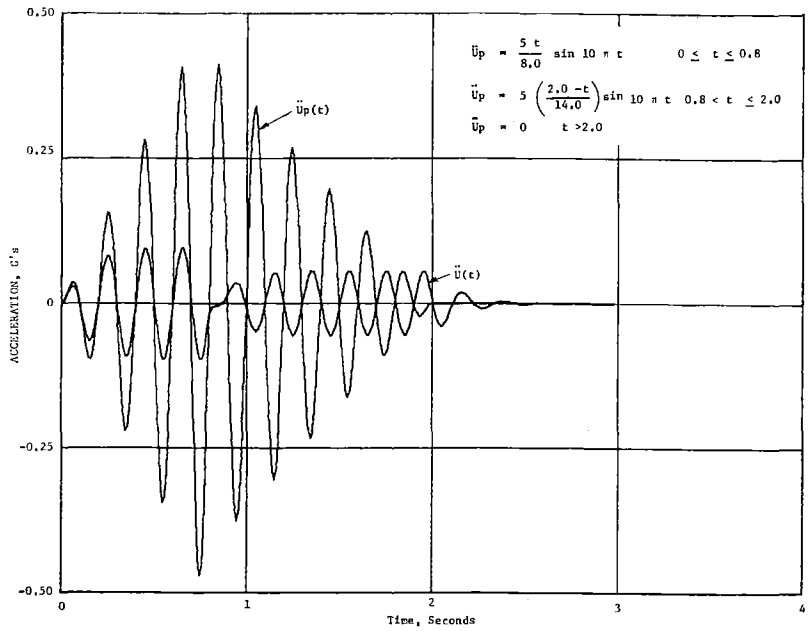

Fig. 5 The acceleration response of a single mass system weighing 475,000 slugs to a ramp sinusoidal function with a 5 cps is shown. The natural frequency of the system is 5.0 cps and the ground shear wave velocity was taken to be 1000 fps.

soils considered. It must be emphasized that for the seismic design of the structure only the spectrum value at the natural frequency of the structure is meaningful. Thus, for computations made with a natural frequency of 4.06 cps, only the spectrum values at this frequency are needed to calculate shock loads of the containment structure. Thus the significance of interaction effects on response spectra can be evaluated by comparing values at the two frequencies of 4.06 cps and 5.0 cps. These values are also listed on Table 1. As observed from both Fig. 6 and Table 1, the largest interaction effects occur when the structure is tuned

Table 1 Spectrum response to the ramp sine function

Soil shear wave velocity fps	Structure fixed base frequency, cps 4.06	5.0
∞ [a]	1.27 *g*	7.18 *g*
500	0.52 *g*	0.62 *g*
1000	0.67 *g*	1.01 *g*
2000	0.87 *g*	2.12 *g*

[a] Spectrum values are those calculated for the ground motion without a structure.

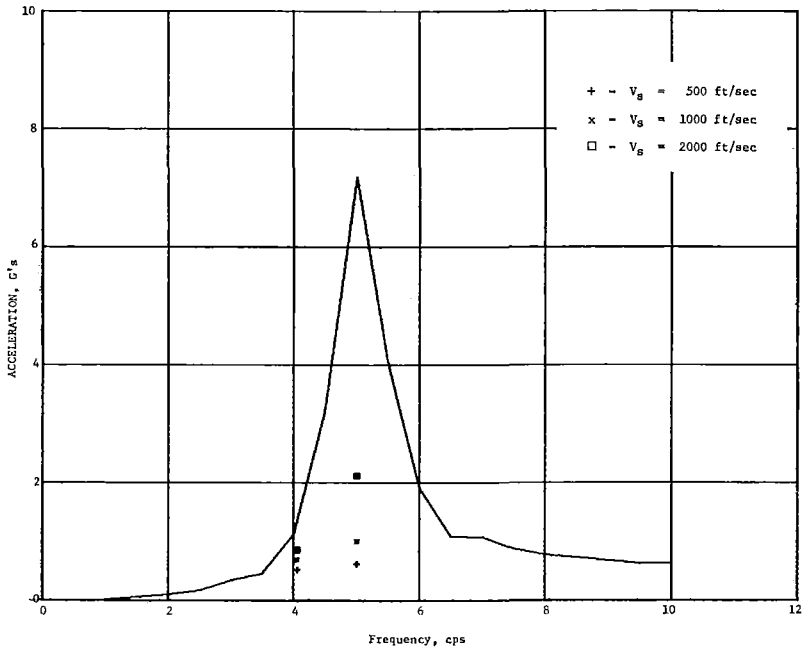

Fig. 6 The acceleration response spectrum for a sinusoidal ramp function is shown as a solid line. The response of one mass dynamic models of reactor power plants with natural frequencies of 4.06 cps and 5 cps for three soil shear wave velocities (500 fps, 1000 fps, and 2000 fps) show the spectrum from interaction effects.

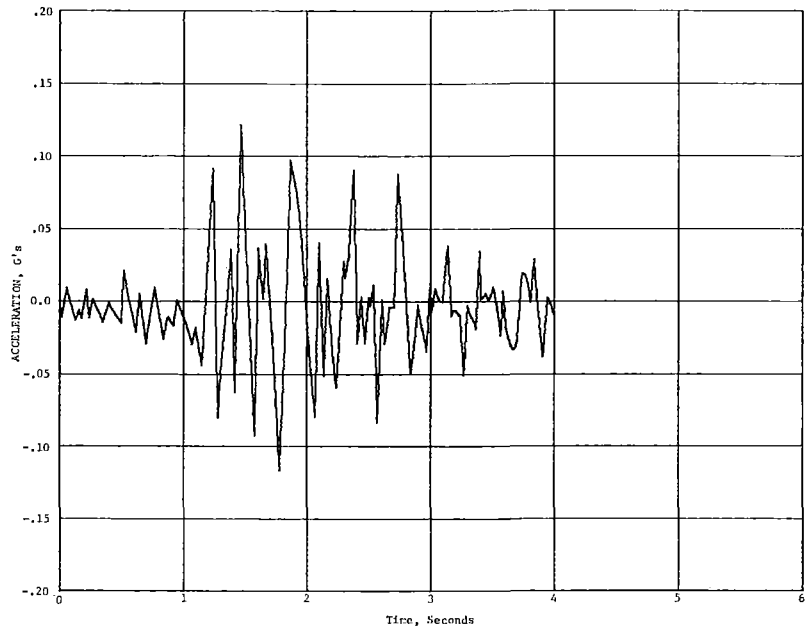

Fig. 7 East-west ground acceleration recorded at Golden Gate Park during the March, 1957, San Francisco earthquake

to the frequency of the prescribed function. In this case, interaction effects reduced the spectra from a factor of 11–3.3, depending upon the ground stiffness. At a frequency of 4.06 cps, these factors varied from 2.4–1.5.

The second free-field ground acceleration used in the numerical work is based on the Mar., 1957, San Francisco earthquake [31]. The first four seconds of the east-west motion recorded at Golden Gate Park (Fig. 7) is used as input. The spectrum response of this motion is presented as a solid line in Fig. 9.

Base foundation accelerations are computed for structures with fixed-base frequencies of 4.06 cps, 4.44 cps and 4.75 cps. The three soil shear wave velocities (500 fps, 1000 fps, and 2000 fps) are also used in these computations. Thus a total of nine problems are studied. A typical calculated foundation acceleration is shown in Fig. 8. Spectrum computations are shown in Fig. 9. The solid line is the response of the assumed earthquake motion. Spectra determined from the calculated base response are shown for the three soil stiffnesses. These values are also tabulated in Table 2. Interaction effects reduce spectra from a factor of 5.6–1.6. Furthermore the largest percentage reductions occur at the peak of the response spectrum (4.44 cps). Thus in-

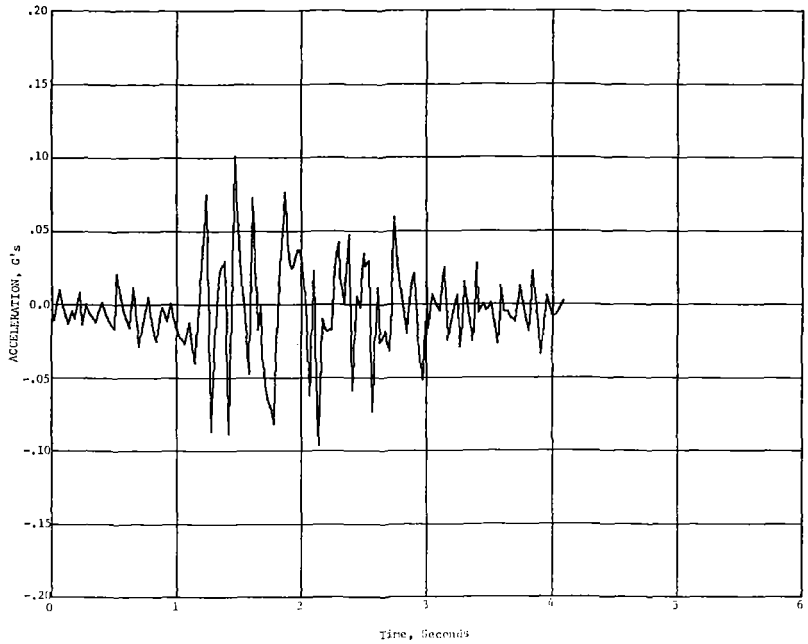

Fig. 8 Ground acceleration at the base of one mass structure with a natural frequency of 4.06 cps and a shear wave velocity of 1000 using the Golden Gate east-west ground motion

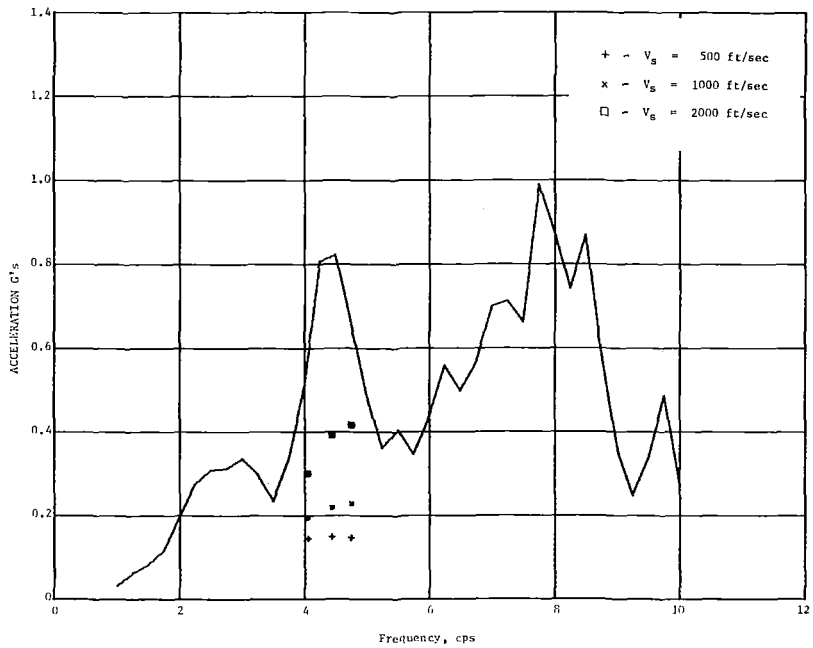

Fig. 9 The acceleration response spectrum for the east-west ground motion recorded at Golden Gate Park during the March, 1957, earthquake is shown as a solid line. The spectrum response of one mass models of reactor power plants with natural frequencies of 4.06 cps, 4.44 cps, and 4.75 cps are shown for three soil shear wave velocities (500 fps, 1000 fps, and 2000 fps).

Table 2 Spectrum response for earthquake motions

Soil shear wave velocity fps	Structure fixed base frequency, cps 4.06	4.44	4.75
∞ [a]	0.59 *g*	0.84 *g*	0.66 *g*
500	0.15 *g*	0.15 *g*	0.15 *g*
1000	0.19 *g*	0.22 *g*	0.23 *g*
2000	0.30 *g*	0.39 *g*	0.42 *g*

[a] Spectrum values are those calculated for the ground motion without a structure.

teraction with the ground tended to level out the free-field spectrum response.

The last parametric study is based on a dynamic model of the Alexander building which has been described previously. This building, which also has been subjected to the earthquake shown in Fig. 7, is studied with three modes of vibration. The calculated foundation acceleration for a ground with a 1000 fps shear wave velocity is shown in Fig. 10. After plotting the results of these it was found that acceleration amplitudes are still large at 4 sec. For the case in which a shear wave velocity of 2000 fps was specified, the second mode of vibration can be seen in the

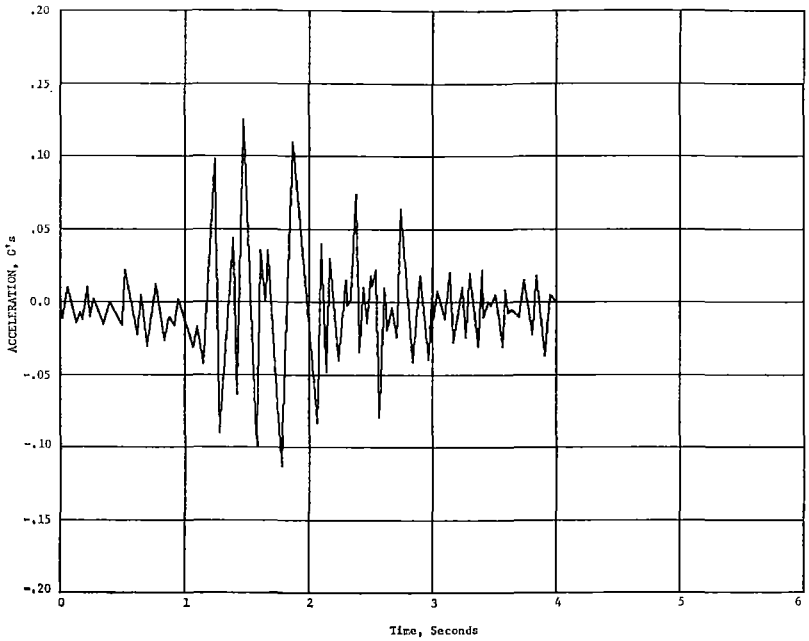

Fig. 10 The response of the Alexander building to the east-west ground acceleration recorded at Golden Gate Park during the March, 1957, San Francisco earthquake. The shear wave velocity of the ground was taken to be 1000 fps.

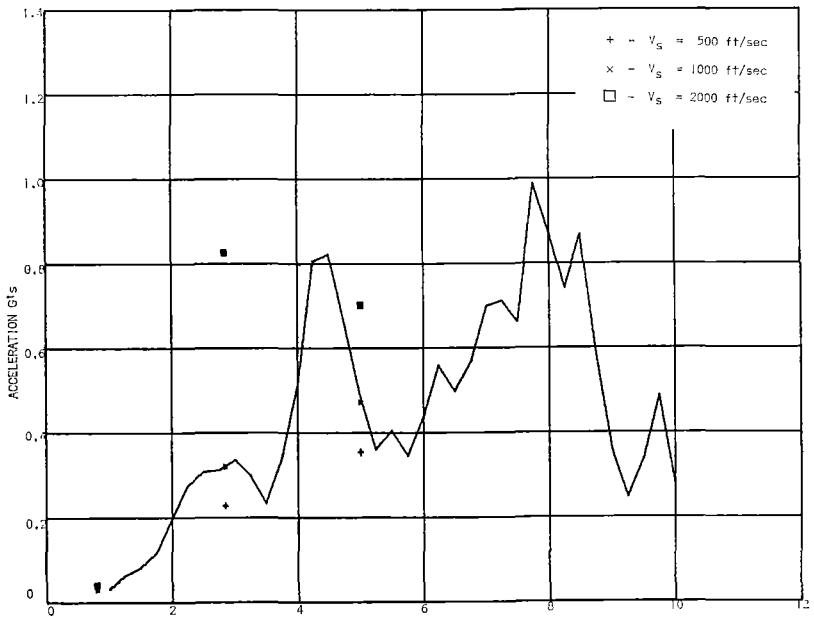

Fig. 11 The acceleration response spectrum for the east-west ground motion recorded at Golden Gate Park during the March, 1957, earthquake is shown as a solid line. The spectrum response of the first three modes of vibration of the Alexander building are plotted (0.8 cps, 2.86 cps, and 5 cps) for the three soil shear wave velocities.

latter portion of the graph. Peak spectrum values which are tabulated in Table 3 and plotted in Fig. 11 occur late in time ($3^1/_2$ to 4 sec). Thus, if time responses are computed for longer periods, calculated spectrum values would probably increase. It should be noted that reductions in spectrum values from interaction effects for this structure occur for the softest soil. For the stiffest soil (b = 2000 fps) spectra values of all modes are increased above free wave spectra. Based upon this limited study of a more conventional building structure, it appears that interaction effects do not always reduce lateral foundation

Table 3 Spectrum response of the Alexander building

Soil shear wave velocity fps	Modes of vibration Mode 1 0.8 cps	Mode 2 2.85 cps	Mode 3 5.0 cps
∞ [a]	0.025	0.335	0.486
500	0.042	0.230	0.358
1000	0.031	0.321	0.473
2000	0.042	0.827	0.721

[a] Spectrum values are those calculated for the ground motion without a structure.

spectra. At times base response spectra are increased. The lack of radiation of energy into the soils is the primary reason for this increase for the structure studied. However, it should be pointed out that rocking effects have not been considered. Rocking spectrum input will also be significant for tall structures. Conclusions made from the study of the Alexander building are similar to those made by Parmalee [16].

Conclusions

By making use of normal mode theory and the solution of a half-space problem in which displacements are caused by a shear stress varying arbitrarily with time over an area symmetric about the origin, lateral interaction between a structure and the half space can be expressed by an integral equation of the Volterra type. Foundation accelerations can be computed with a digital computer program which solves this equation by numerical iteration at each time interval. Spectrum responses can also be computed from these foundation accelerations.

Results of spectrum calculations show that reductions in lateral shock spectra caused by interaction effects are significant and must be accounted for in the design of heavy stiff structures. Peaks in the free-field response spectra of earthquakes are reduced more than other values. As shown in Fig. 9, interaction effects from these structures tend to level out the response curves. For conventional multistory structures such as the Alexander building which is studied, interaction effects will, at times, increase spectrum values above the free-field spectrum. In conclusion it can be stated that significant reductions in the lateral spectrum response can be expected from interaction of the building and ground for low heavy stiff structures. For flexible tall buildings interaction may slightly increase the base spectrum response and the resulting lateral accelerations.

Acknowledgment

The support for this investigation was provided by the United States Atomic Energy Commission under Contract No. AT-(40-1)3822. In particular the authors are grateful to R. R. Newton of the Reactor Development and Technology branch for his suggestions.

References

1 Jacobsen, L. S., "Natural Periods of Uniform Cantilever Beams," *ASCE Transactions*, Vol. 104, 1939, pp. 402–439.

2 Biot, M. A., "Analytical and Experimental Methods in Engineering Seismology," *ASCE Transactions*, Vol. 108, 1943, p. 365.

3 Scavuzzo, R. J., and Raftopoulos, D., "Literature Review of Structure-Foundation Interaction," USAEC Contract No. AT-(40-1)-3822, Technical Report No. 1, The Research Foundation, University of Toledo, Oct. 1968.

4 O'Hara, G. J., and Cunniff, P. F., "Elements of Normal Mode Theory," NRL Report 6002, Nov. 1963.

5 Belsheim, R. O. and O'Hara, G. J., "Shock Design of Shipboard Equipment, Part 1-Dynamic Design Analysis Method," NRL Report 5545, 1960.

6 Cunniff, P. F., and O'Hara, G. J., "Normal Mode Theory for Three-Dimensional Motion," NRL Report 6170, Jan. 1965.

7 Blake, R. E., and Swick, E. S., "Dynamics of Linear Elastic Structures," NRL Report 4420, Oct. 1954.

8 O'Hara, G. J., "Notes on Dynamics of Linear Elastic Structures," NRL Report 5387, Oct. 1959.

9 O'Hara, G. J., and Belsheim, R. O., "Shock Design of Shipboard Equipment—Part 11-i, Interim Design Inputs for Submarine Equipments," NRL Letter Report 6262-396A, confidential, Sept. 1960.

10 BuShips, "Shock Design of Shipboard Equipment, Interim Design Inputs for Submarine and Surface Ship Equipment," NavShips 250-423-31, confidential, Feb. 1963.

11 O'Hara, G. J., and Belsheim, R. O., "Interim Design Values for Shock Design of Shipboard Equipment," NRL Memorandum Report 1396, confidential, Feb. 1963.

12 Belsheim, R. O., and Blake, R. E., "Effect of Equipment Dynamic Reaction on Shock Motion of Foundations," NRL Report 5009, confidential report, unclassified title, Oct. 1957.

13 O'Hara, G. J., "Effect Upon Shock Spectra of the Dynamic Reaction of Structures," NRL Report 5236, Dec. 1958, published in SESA V18, 1961.

14 O'Hara, G. J., "Impedance and Shock Spectra," *Journal of the Acoustical Society of America*, Vol. 31, Oct. 1959, pp. 1300–1303.

15 O'Hara, G. J., "Shock Spectra and Design Shock Spectra," NRL Report 5386, Nov. 1959.

16 Parmalee, R. A., "Building-Foundation Interaction Effects," *Proceedings ASCE*, JEMD, Apr. 1967, pp. 131–152.

17 Luco, J. E., "Dynamic Interaction of a Shear Wall With the Soil," *Proceedings ASCE*, JEMD, Apr. 1969, pp. 333–346.

18 Agabein, M. E., Parmalee, R. A., and Lee, S. L., "A Model for the Study of Soil-Structure Interaction," 8th Congress of International Association for Bridge and Structural Engineering, New York, September 12, 1968.

19 Bycroft, G. N., "Forced Vibrations of a Rigid Circular Plate on a Semi-Infinite Elastic Space and on an Elastic Stratum," *Philosophical Transactions of the Royal Society*, London, Series A, Vols. 248, 948, Jan. 1956, pp. 327–368.

20 Arnold, R. N., Bycroft G. N., and Warburton, G. B., "Forced Vibrations of a Body in an Elastic Solid," JOURNAL OF APPLIED MECHANICS, Vol. 22, TRANS. ASME, Vol. 77, Sept. 1955, pp. 392–400.

21 Scavuzzo, R. J., "Foundation-Structure Interaction in the Analysis of Wave Motions," *Bulletin of the Seismological Society of America*, Vol. 57, 1967, pp. 735–746.

22 Scavuzzo, R. J., "Interaction Between Equipment Structures and Underwater Shock Waves," *The Shock and Vibration Bulletin*, Supplement No. 39, Naval Research Laboratory, Washington, D. C., Apr. 1969.

23 Flitman, L. M., "Dynamic Problems of the Die on an Elastic Half Space," *Prikladnaya Mathematika i Mechanika*, Vol. 23, No. 4, 1959, pp. 997–1008.

24 Sneddon, I. N., *Fourier Transforms*, McGraw-Hill, New York, 1951, pp. 444–449.

25 Chao, C. C., "Dynamical Response of an Elastic Half Space to Tangential Surface Loadings," JOURNAL OF APPLIED MECHANICS, Vol. 27, No. 3, TRANS. ASME, Vol. 82, Series E, Sept. 1960, pp. 559-567.

26 Lamb, H., "On the Propagation of Tremors Over the Surface of an Elastic Solid," *Philosophical Transactions of the Royal Society*, London, Series A, Vol. 203, 1904, pp. 1–42.

27 Scavuzzo, R. J., Bailey, J. L., and Raftopoulos, D. D., "Lateral Structure-Foundation Interaction of Nuclear Power Plants During Earthquake Loading," USAEC Contract No. AT-(40-1)3822, Technical Report No. 2, The Research Foundation, The University of Toledo, Aug. 1969.

28 Scavuzzo, R. J., Raftopoulos, D. D., and Bailey, J. L., "Lateral Structure-Foundation Interaction of Nuclear Power Plants With Large Base Masses," USAEC Contract No. AT-(40-1)3822, Technical Report No. 3, The Research Foundation, University of Toledo, Sept. 1969.

29 Blume, J. A., "Period Determination and Other Earthquake Studies of a Fifteen-Story Building," *Proceedings of the First World Conference on Earthquakes*, June 1956, pp. 11-1 to 11-27.

30 Clough, R. W., "Dynamic Effects of Earthquakes," ASCE Structure Division, ST 4, 1960, pp. 847–863.

31 Holmes and Narver, Inc., "Nuclear Reactors and Earthquakes," TID-7024, Aug. 1963, p. 1.1E; available from the United States Department of Commerce.